Nature of Magnetic Dynamo Growth in the High Magnetic Reynolds Number Limit

Charles Reyl, Thomas M. Antonsen, Jr.,* and Edward Ott*,†
Institute for Plasma Research and Department of Physics, University of Maryland, College Park, Maryland 20742
(Received 19 December 1995)

It has been conjectured that essential features of fast kinematic magnetic dynamos in the presence of small magnetic diffusivity can be extracted from the ideal (i.e., diffusionless) kinematic dynamo equation. In particular, predictions concerning the cancellation exponent, the dynamo growth rate, and the growth of moments of the magnetic field in the nonideal case can be made based on the ideal dynamics. This paper presents the first confirmation of these predictions by numerical computations on a spatially smooth chaotic flow at very high magnetic Reynolds number.

PACS numbers: 47.65.+a, 05.45.+b, 47.52.+j

Fast dynamo action [1] refers to the exponential growth of magnetic field perturbations to a flowing electrically conducting fluid in the limit of vanishing resistivity. Flows having this property are commonly thought to be responsible for the formation of the large magnetic fields found in [1,2] planets with liquid cores, the outer layers of stars, interstellar gas making up the gaseous disk of the galaxy, etc. The problem of determining dynamo action is referred to as the kinematic magnetic dynamo problem [1–25], when attention is restricted to the initial stage of the dynamo in which the magnetic field is small enough that the reaction on the flow field provided by the Lorentz force can be neglected. The equation describing the effect of a prescribed incompressible flow $\boldsymbol{v}(\boldsymbol{x},t)$ $(\nabla \cdot \boldsymbol{v} = 0)$ on a magnetic field $\boldsymbol{B}(\boldsymbol{v},t)$ reads

$$\partial \boldsymbol{B}/\partial t + \boldsymbol{v} \cdot \nabla \boldsymbol{B} = \boldsymbol{B} \cdot \nabla \boldsymbol{v} + R_m^{-1}\nabla^2 \boldsymbol{B}, \qquad (1)$$

where $\boldsymbol{v}$ has been normalized to a typical velocity of the flow v_0, and $\boldsymbol{x}$ to a typical length scale of the flow L_0. Note that the term $R_m^{-1}\nabla^2\boldsymbol{B}$ represents magnetic field diffusion. The dimensionless magnetic Reynolds number is defined as $R_m = (4\pi\sigma L_0 v_0)/c^2$, where σ is the electrical conductivity of the fluid. For example, the magnetic Reynolds number for the Sun is of order 10^8. It is therefore of interest to investigate the limit where R_m approaches infinity in Eq. (1). We may start by setting $R_m = \infty$ as if the fluid were perfectly conducting. Eq. (1) then reduces to the following ordinary differential equation,

$$d\tilde{\boldsymbol{B}}/dt = \tilde{\boldsymbol{B}} \cdot \nabla \boldsymbol{v}, \qquad (2)$$

where $d/dt = \partial/\partial t + \boldsymbol{v} \cdot \nabla$, and $\tilde{\boldsymbol{B}}$ denotes the magnetic field when diffusion is absent. Note that by replacing $\tilde{\boldsymbol{B}}$ by $\boldsymbol{\delta}$ in Eq. (2), where $\boldsymbol{\delta}$ is the infinitesimal separation between two nearby orbits, the time-evolution equation for $\boldsymbol{\delta}(t)$ is recovered: $d\boldsymbol{\delta}/dt = \boldsymbol{\delta} \cdot \nabla \boldsymbol{v}$. The equivalence of the equations for $\tilde{\boldsymbol{B}}$ and $\boldsymbol{\delta}$ allows one to reduce the diffusion-free kinematic dynamo problem to the study of the dynamical properties of the underlying flow. It also implies that only flows providing exponential stretching are candidates for fast dynamos [4,7,8,11,25]. In particular, we call the flow $\boldsymbol{v}(\boldsymbol{x},t)$ chaotic if $d\boldsymbol{x}/dt = \boldsymbol{v}(\boldsymbol{x},t)$ has ergodic regions with a positive Lyapunov exponent, $\bar{h} = \lim_{t\to\infty} t^{-1}\ln[|\boldsymbol{\delta}(t)|/|\boldsymbol{\delta}(0)|] > 0$, for typical $\boldsymbol{\delta}(0)$.

Although chaotic flows seem to be very good candidates for fast dynamo activity, some care should be exercised in drawing conclusions from the ideal case to the diffusive case, because the limit $R_m \to \infty$ is a highly singular one. This statement is illustrated by noting that the smallest scale ϵ_* for magnetic field variations is given by [6] $\epsilon_* \sim R_m^{-1/2}$. Thus, although $1/R_m$ is small, $R_m^{-1}\nabla^2\boldsymbol{B}$ in (1) is not, and it is still a problem to relate the solutions of Eq. (1) at very large finite R_m and (2).

In what follows we test several fundamental issues concerning dynamo action in the large R_m limit using numerical computations of (1) for a model dynamo flow. Because of the large magnetic Reynolds number achieved and because of other favorable properties of the flow we use, our computations are able to address issues not resolvable in previous computations. In particular, we shall focus on the effect of small diffusivity on the cancellation exponent, on the magnetic flux growth rate, and on the time evolution of the magnetic moment growth rates. Our numerical computations [26] are done at $R_m = 10^5$ using an incompressible, smooth, three-dimensional, chaotic flow of the form $\boldsymbol{v}(x,y,t) = \boldsymbol{x}_0\tilde{v}_x(y)f(t) + \boldsymbol{y}_0\tilde{v}_y(x)f(t - T/3) + z_0\tilde{v}_z(x)f(t - 2T/3)$, where $f(t)$ is a periodic function with period T, $f(t) = 0$ for $T/3 + nT < t < (n+1)T$ with n integer, so that the flows in the x, y, and z directions are turned on sequentially. Also, $f(t)$ is normalized: $\int_0^T f(t)dt = 1$. This flow has two features that allow very efficient computation. The first one is that the flow is independent of one of the spatial coordinates (z, for instance). Equation (1) is then separable in z, and the magnetic field is given a harmonic z dependence, $\boldsymbol{B} \sim \exp(ik_z z)$. Consequently, all calculations can be performed on a two-dimensional surface. Dynamos generated by this type of flow are called *quasi-two-dimensional* dynamos [3,15,23,24]. The second feature of our flow is its sequential character, which has the effect of decoupling the computations along the x and y directions in the three phases of flow during each period. The integration of the Fourier representation of Eq. (1) over any third of a pe-

 0031-9007/96/76(13)/2270(4)$10.00 © 1996 The American Physical Society

riod T can then be performed independently for each set of modes, rending the computation effectively one dimensional. [This feature also makes the flow amenable to parallel computation (not used here).]

The chaotic dynamics generated by this flow can be analyzed by integrating $\boldsymbol{v}(x, y, t)$ over one period T. We obtain a three-dimensional volume-preserving map relating $\boldsymbol{x}$ at $t = nT$ to $\boldsymbol{x}$ at $t = n(T + 1)$: $\boldsymbol{x}_{n+1} = \boldsymbol{M}(\boldsymbol{x}_n)$. Note that the map does not depend on the specific form of $f(t)$. We choose $\tilde{\boldsymbol{v}}$ to be of the form $\tilde{v}_x = U_x \sin(K_y y + \theta_x)$, $\tilde{v}_y = U_y \sin(K_x x + \theta_y)$, $\tilde{v}_z = U_z \sin(K_x x + \theta_z)$. Note that $\tilde{\boldsymbol{v}}$ and its convolution with the magnetic field have very simple Fourier transforms. We also find it convenient to make the phase angles θ_x, θ_y, and θ_z time dependent such that they are independent random variables, constant in each period $nT \leq t < (n + 1)T$. In this case, we take the distributions of θ_x, θ_y, and θ_z to be uniform on the interval $[0, 2\pi]$, and we reset them simultaneously at $t = nT$. These random phases ensure that there are no Kolmogorov-Arnold-Moser (KAM) tori and that orbits of $\boldsymbol{M}$ are ergodic over all space even at low values of the amplitudes U_x, U_y, and U_z. Small amplitudes keep the largest Lyapunov exponent reasonably small. The latter quantity provides a rough order of magnitude estimate of the growth of the magnetic field and should not be too large if we want to clearly observe the transition from the nondiffusive growth phase (discussed subsequently) to the diffusive growth phase. We believe that our results obtained with this choice of random phases $\boldsymbol{\theta}$ are a good qualitative indication of behavior in general flows with complicated time dependence.

In most previous numerical dynamo calculations using steady or time-periodic flows, much of the spatial grid was occupied by KAM tori. Since fast dynamo action is due to the chaotic regions, much of the grid is, in a sense, wasted. Another way of saying this is that, since the active region is smaller than the full region, the effective Reynolds number is reduced (if we regard the relevant length scale as the width of the chaotic layer, rather than the size of the full region). Such considerations do not apply for random flows since KAM surfaces are necessarily absent.

It has been conjectured in Refs. [7,10] that the growth rate of the magnetic flux through a macroscopic surface S, $\boldsymbol{\Phi}_S(t) = \int_S \boldsymbol{B} \cdot d\boldsymbol{A}$, is invariant when taking the limit $R_m \to \infty$. This can be understood by considering the scale over which diffusion is active. The role of small diffusion is to smooth and rearrange spatial variations of $\boldsymbol{B}$ over lengths of the order $R_m^{-1/2}$ in a characteristic time interval $1/\gamma_{\max}(R_m)$, where $\gamma_{\max}(R_m)$ is the growth rate of the fastest growing mode. For large R_m, this scale will be small compared to the dimensions of S, and the exponential growth of $\boldsymbol{\Phi}_S(t)$ is thus expected to be R_m independent. The same reasoning applies to the cancellation exponent κ [18,19,27].

A formula relating the flux growth rate to the stretching properties of the flow and the cancellation exponent has been derived on heuristic grounds in Ref. [19]. In the case of a conservative z-independent flow, the product of the eigenvalues of its Jacobian is one, and the eigenvalue λ_2 associated with the eigenvector in the z direction is also one. Therefore, the two remaining eigenvalues $\lambda_1 > \lambda_3$ are the inverse of each other, and the stretching properties of the flow are uniquely determined by the largest growth factor λ_1. Hence, the formula reads

$$\gamma_* = \lim_{n\to\infty} n^{-1} \ln\langle \lambda_1^{1-\kappa} \rangle, \tag{3}$$

where $\lambda_1(\boldsymbol{x}, n) = |\boldsymbol{\delta}(n)|/|\boldsymbol{\delta}(0)|$ maximized over $\boldsymbol{\delta}(0)$ and the average $\langle \cdots \rangle$ is taken over the ergodic region. A distribution function $P(h, n)$ [28] of the finite-time Lyapunov exponent $h(\boldsymbol{x}, n) = n^{-1} \ln \lambda_1(\boldsymbol{x}, n)$ for randomly chosen $\boldsymbol{x}$ can be obtained numerically [26,29]. For our flow, $P(h, n)$ is well approximated by a Gaussian of the form $P(h, n) \approx \sqrt{nG''(\bar{h})/2\pi}\, \exp[-(1/2)nG''(\bar{h})(h - \bar{h})^2]$, where $[nG''(\bar{h})]^{-1/2}$ is the standard deviation of h. The average in Eq. (3) can then be performed, $\langle \lambda_1^{1-\kappa} \rangle \cong \int P(h, n) \exp[(1 - \kappa)nh]dh$, and γ_* is obtained in terms of κ, $\bar{h}$ and $G''(\bar{h})$:

$$\gamma_* = (1 - \kappa)\bar{h} + (1 - \kappa)^2/2G''(\bar{h}). \tag{4}$$

Table I lists the results for the following parameter values of the flow: $U_x = U_y = 1.6$, $U_z = 1$, and $K_x = K_y = 1$. The harmonic z dependence of the dynamo solution is arbitrarily set to $k_z = 1$, and we note that the growth rate and cancellation exponent depend on k_z (this dependence will be reported elsewhere). The results in the first two columns (corresponding to κ and γ_*) are reported without giving descriptions of details of the computations which will be given in a longer publication [26]. We wish to note, however, that *the cancellation exponent is the same to within numerical accuracy for both ideal and diffusive cases.* Further, the results for γ_* in Table I show that *the flux growth rates with and without diffusion are in*

TABLE I. Cancellation exponent κ, flux growth rates γ_*, initial (or ideal) moments growth rates $\tilde{\gamma}_\nu$, and postdiffusion moments growth rates γ_ν. The predicted values are calculated using the numerically obtained balues $G''(\bar{h}) = 3.366$, $\bar{h} = 0.313$, and $\kappa = 0.47 \pm 0.01$.

	κ	γ_*	$\tilde{\gamma}_0$	$\tilde{\gamma}_1$	$\tilde{\gamma}_2$	γ_0	γ_1	γ_2
Predicted	$\cdots$	0.208 ± 0.01	0.313	0.462	0.610	0.208	0.208	0.208
Measured ($R_m = \infty$)	0.47 ± 0.01	0.20 ± 0.05	0.32	0.48	0.61	$\cdots$	$\cdots$	$\cdots$
Measured ($R_m = 10^5$)	0.46 ± 0.03	0.21 ± 0.05	0.34	0.45	0.57	0.19	0.17	0.16

very good agreement and agree with the theoretical prediction [Eq. (4)] when the numerically estimated values of $\bar{h}$, $G''(\bar{h})$, and the cancellation exponent ($\kappa = 0.47 \pm 0.01$) are used.

As an example showing the quality of numerical results achievable with our flow computations, we provide, in what follows, a detailed discussion of the growth of moments of the magnetic field (columns 3–8 of Table I).

Let $F_\nu(n)$ be the νth root of the νth moment of the modulus of the magnetic field at time n:

$$F_\nu(n) \equiv \left(S^{-1} \int_S |\boldsymbol{B}(x, y, 0; n)|^\nu dx dy \right)^{1/\nu}, \qquad \nu \neq 0\,, \tag{5}$$

where S is a two-dimensional surface in the (x, y) plane. $F_1(n)$ can be interpreted as the flux density without cancellation and $F_2(n)$ as the square root of the magnetic energy density. The limit $\nu \to 0$ yields $F_0(n) = \exp[S^{-1} \int_S \ln |\boldsymbol{B}(x, y, 0; n)| dx dy]$. Let γ_ν denote the exponential growth rate of $F_\nu(n)$. Because of the equivalence between the ideal magnetic field $\tilde{\boldsymbol{B}}(\boldsymbol{x})$ and the infinitesimal displacement $\boldsymbol{\delta}(\boldsymbol{x})$, we note that $\tilde{\gamma}_0$ is the Lyapunov exponent $\bar{h}$ and that $\tilde{\gamma}_1$ is the topological entropy of the underlying flow, where $\tilde{\gamma}_\nu$ is the growth rate of the νth moment of the ideal magnetic field. [Here $\tilde{\gamma}_\nu$ is obtained by replacing F_ν by $\tilde{F}_\nu$, where $\tilde{F}_\nu$ is given by Eq. (5) with $\tilde{\boldsymbol{B}}$ replacing $\boldsymbol{B}$.]

Contrary to the magnetic flux, the moments $F_\nu(n)$ exhibit a transition at the onset of diffusion, i.e., when the smallest variation scale $\epsilon_*(n)$ reaches the diffusive scale [13]. While the diffusion term is still negligible, the moments exhibit different growth rates as a function of ν with $\gamma_\nu = \tilde{\gamma}_\nu$. However, when diffusion sets in, the smallest scale becomes time independent ($\epsilon_* \sim R_m^{-1/2}$), and we consequently expect the growth rates of the moments to all collapse to the dynamo growth rate [13] independent of ν: $\gamma_\nu = \gamma_{\max}(R_m)$.

The moment growth rates before the onset of diffusion $\tilde{\gamma}_\nu$ can be calculated using the probability distribution of finite time Lyapunov exponents, $F_\nu(n) \sim \langle \lambda_1^\nu(\boldsymbol{x}, n) \rangle^{1/\nu} = [\int P(h, n) \exp(n\nu h) dh]^{1/\nu}$. Using again the Gaussian approximation for $P(h, n)$, the growth rates $\tilde{\gamma}_\nu$ read

$$\tilde{\gamma}_\nu = \bar{h} + \nu / 2G''(\bar{h})\,. \tag{6}$$

This approximation is in excellent agreement with numerically obtained growth rates. See Table I and the plot in Fig. 1(a).

The times τ_ν at which the diffusion starts to affect the growth of the different moments can be estimated in the following way. As ν increases, large fields acquire a greater influence in determining the value of the νth moment. Larger fields are the ones whose flux lines experienced a larger amount of stretching and are therefore located in regions of sharper variation ($\lambda_3 = \lambda_1^{-1}$) characterized by a smaller local scale $\epsilon(\boldsymbol{x}, n)$. Thus, we expect high moments to feel the effect of diffusion

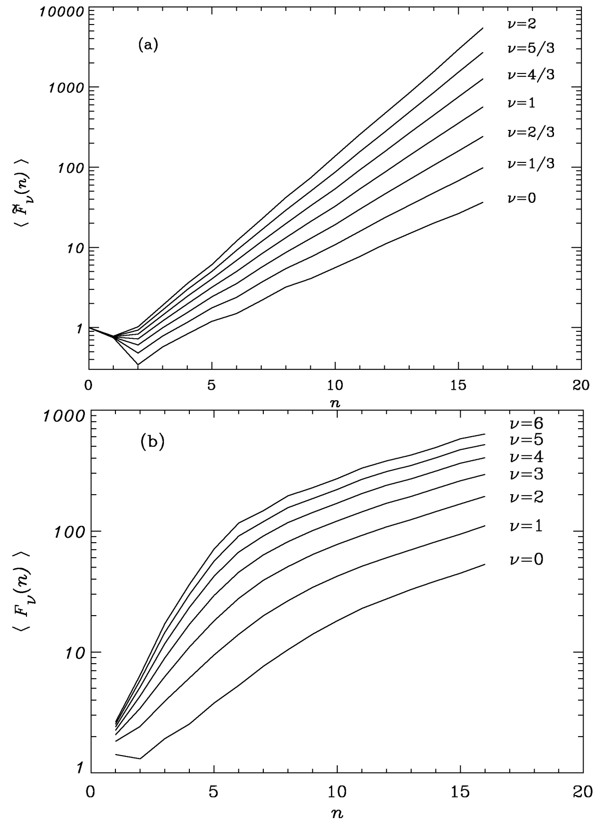

FIG. 1. (a) The time evolution of $\langle \tilde{F}_\nu(n) \rangle$, $\nu = 0, 1/3, 2/3, \ldots, 2$ is plotted on a logarithmic scale. The growth rates $\tilde{\gamma}_\nu$ are the slopes of the fits to the corresponding straight lines. (b) The time evolution of $\langle F_\nu(n) \rangle, \nu = 0, 1, \ldots, 6$ is plotted on a logarithmic scale. The growth rates γ_ν are the slopes of the fits to the corresponding straight lines. The magnetic Reynolds number R_m is 10^5.

faster than low moments, or, in other words, the times τ_ν at which the moment feels the effect of diffusion are expected to decrease as ν increases. Using the equivalence $\int_S |\boldsymbol{B}(n)|^\nu dx dy \sim \langle \lambda_1^\nu(\boldsymbol{x}, n) \rangle$, we associate $F_\nu(n)$ to a magnetic field whose strength is given by the average stretching $\langle \lambda_1^\nu \rangle^{1/\nu}$. The variation scale attached to this larger field is given by $\epsilon_\nu = L_0 \langle \lambda_1^\nu \rangle^{-1/\nu}$. Setting $\epsilon_\nu = L_0 / \sqrt{R_m}$, we obtain the diffusion transition times $\tau_\nu \approx \ln R_m / [2\bar{h} + \nu / G''(\bar{h})] = \ln R_m / (2\tilde{\gamma}_\nu)$. The times τ_ν coincide roughly with the end of the transition from the ideal growth phase to the diffusive growth phase on the plot of Fig. 1(b).

For the ideal case in Fig. 1(a), the different moments of $\tilde{\boldsymbol{B}}$ clearly grow at different rates. Table I lists the growth rates for the ideal case and corresponding predictions from Eq. (6). The agreement between the numerically measured and the predicted values is very good. The situation with diffusion in Fig. 1(b) is radically different. After an initial phase similar to what is observed in the ideal case, a transition occurs at which the growth rates γ_ν collapse approximately on the flux growth rate γ_*. The growth rates γ_0, γ_1, and γ_2 are listed in Table I. These values are close to each other compared to their much greater differences before diffusion sets in [30].

In conclusion, in this paper we present numerical results on a high magnetic Reynolds number dynamo flow and use these results to investigate several outstanding issues in dynamo theory. In particular, we find the following: (i) The flux growth and cancellation exponents calculated at $R_m = 10^5$ from (1) and at infinite R_m from (2) are approximately the same. (ii) A formula [Eq. (3)] relating the large R_m dynamo growth rate to the cancellation exponent is found to hold to within the numerical accuracy obtained. (iii) Growth of magnetic field moments occurs in two stages and is in accord with the calculations based on the finite-time Lyapunov exponent distribution.

This work was supported by the Office of Naval Research (Physics). The numerical computations reported in this paper were supported in part by a grant from the W. M. Keck Foundation.

*Also at Department of Electrical Engineering.
†Also at Institute for Systems Research.

[1] S. I. Vainshtein and Ya. B. Zeldovich, Sov. Phys. Usp. **15**, 159 (1972); Ya. B. Zeldovich and A. A. Ruzmaikin, Sov. Phys. JETP **51**, 493 (1980).

[2] E. N. Parker, *Cosmical Magnetic Fields: Their Origin and Activity* (Oxford University Press, Oxford, 1979).

[3] S. Childress and A. D. Gilbert, *Stretch, Twist, Fold: The Fast Dynamo* (Springer-Verlag, Berlin, to be published).

[4] V. I. Arnold, Ya. B. Zeldovich, A. A. Ruzmaikin, and D. D. Sokolov, Sov. Phys. JETP **54**, 1083 (1981).

[5] D. Galloway and U. Frisch, Geophys. Astrophys. Fluid Dyn. **36**, 53 (1986).

[6] H. K. Moffat and M. R. Proctor, J. Fluid Mech. **154**, 493 (1985).

[7] J. Finn and E. Ott, Phys. Fluids **31**, 2992 (1988).

[8] B. J. Bayly and S. Childress, Geophys. Astrophys. Fluid Dyn. **44**, 211 (1988).

[9] B. J. Bayly and S. Childress, Geophys. Astrophys. Fluid Dyn. **49**, 23 (1989).

[10] J. Finn, J. Hanson, I. Kan, and E. Ott, Phys. Rev. Lett. **62**, 2965 (1989).

[11] M. M. Vishik, Geophys. Astrophys. Fluid Dyn. **48**, 151 (1989).

[12] E. Ott and T. M. Antonsen, Phys. Rev. A **39**, 3660 (1989).

[13] J. Finn and E. Ott, Phys. Fluids B **2**, 916 (1990).

[14] J. Finn, J. Hanson, I. Kan, and E. Ott, Phys. Fluids B **3**, 1250 (1991).

[15] D. J. Galloway and M. R. E. Proctor, Nature (London) **356**, 691 (1992).

[16] A. D. Gilbert and B. J. Bayly, J. Fluid Mech. **241**, 199 (1992).

[17] A. D. Gilbert, Philos. Trans. R. Soc. London A **339**, 627 (1992).

[18] Y. Du and E. Ott, Physica (Amsterdam) **67D**, 387 (1993).

[19] Y. Du and E. Ott, J. Fluid Mech. **257**, 265 (1993).

[20] Y.-T. Lau and J. Finn, Phys. Fluids B **5**, 365 (1993).

[21] A. Soward, Geophys. Astrophys. Fluid Dyn. **73**, 179 (1993).

[22] A. D. Gilbert, N. F. Otani, and S. Childress, *Theory of Solar and Planetary Dynamics* (Cambridge University Press, Cambridge, England, 1993).

[23] Y. Ponty, A. Pouquet, and P. L. Sulem, Geophys. Astrophys. Fluid Dyn. **79**, 239 (1995).

[24] F. Cattaneo, E. Kim, M. Proctor, and L. Tao, Phys. Rev. Lett. **75**, 1522 (1995).

[25] I. Klapper and L. S. Young, Commun. Math. Phys. **173**, 623 (1995).

[26] C. Reyl, T. M. Antonsen, and E. Ott, Physics of Plasmas (to be published).

[27] E. Ott, Y. Du, K. R. Sreenivasan, A. Juneja, and A. K. Suri, Phys. Rev. Lett. **69**, 2654 (1992). The cancellation exponent κ provides a measure of singular behavior of the magnetic field associated with rapid spatial alternation in the orientation of the field. Let $\chi(\epsilon, n) = \sum_i |\int_i dxdy\,\boldsymbol{B}(\boldsymbol{x}; n)| / \int_V dxdy |\boldsymbol{B}(\boldsymbol{x}; n)|$, where i denotes a cube from an ϵ grid which covers a cube of volume V and of edge length L. Then, $\kappa = \lim_{\epsilon\to 0} \lim_{n\to\infty} \ln \chi(\epsilon, n)/\ln(L/\epsilon)$. In the case of finite R_m, $\kappa = \lim_{\epsilon\to 0} \lim_{R_m\to\infty} \lim_{n\to\infty} \ln \chi(\epsilon, R_m, n)/\ln(L/\epsilon)$.

[28] See, for example, E. Ott, *Chaos in Dynamical Systems* (Cambridge University Press, Cambridge, England, 1993), and references therein.

[29] See, for example, P. Grassberger, R. Badii, and A. Politi, J. Stat. Phys. **51**, 135 (1988); F. Varosi, T. Antonsen, and E. Ott, Phys. Fluids A **3**, 1017 (1991).

[30] It appears that the numerical values of $\tilde{\gamma}_\nu$ decrease slightly as ν increases. As discussed in [26], this is an artifact of the computation indicative of an insufficiently fine grid which tends to "miss" the most intense magnetic fields located in the regions of most rapid spatial variation.